JACS
JOURNAL OF THE AMERICAN CHEMICAL SOCIETY
Communication
pubs.acs.org/JACS

Light-Induced Proton-Coupled Electron Transfer Inside a Nanocage

Rahul Gera, Ankita Das, Ajay Jha, and Jyotishman Dasgupta*

Department of Chemical Sciences, Tata Institute of Fundamental Research, Mumbai 400005, India

Supporting Information

ABSTRACT: Triggering proton-coupled electron-transfer (PCET) reactions with light in a nanoconfined host environment would bring about temporal control on the reactive pathways via kinetic stabilization of intermediates. Using a water-soluble octahedral Pd_6L_4 molecular cage as a host, we show that optical pumping of host−guest charge transfer (CT) states lead to generation of kinetically stable phenoxyl radical of the incarcerated 4-hydroxy-diphenylamine (1-OH). Femtosecond broadband transient absorption studies reveal that CT excitation initiates the proton movement from the 1-OH radical cation to a solvent water molecule in ∼890 fs, faster than the time scale for bulk solvation. Our work illustrates that optical host−guest CT excitations can drive solvent-coupled ultrafast PCET reactions inside nanocages and if optimally tuned should provide a novel paradigm for visible-light photocatalysis.

Proton-coupled electron-transfer (PCET) reaction forms the chemical basis for carrying out kinetically competent multielectron redox transformations.[1−5] Classically PCET involves instantaneous proton transfer (PT) subsequent to or concerted with a diffusion-limited electron-transfer (ET) step. An exquisite illustration of PCET is prominently found in the catalytic $4e^-/4H^+$ water oxidation reaction carried out by photosystem II.[6−9] The spatial and temporal separation of protons and electrons via PCET in PSII critically governs the energetics of the individual oxidation steps without compromising the chemical integrity of the enzyme. Therefore, an active synthetic control on PCET reactions would be a significant step toward engineering efficient catalytic schemes for artificial photosynthesis.

Molecular systems that beautifully mimic major aspects of the PCET step in photosynthesis have been constructed previously.[10−14] These usually feature extensive covalent chemistry to tag the electron and proton donor−acceptors in the same superstructure.[15,16] Alternately, it has been realized that light-induced PCET could be implemented in simpler designs and potentially could open up new avenues for catalysis. In recent years chemically coupling the excited-state reactivity of organic and metal-based photosensitizers to PCET has been successfully shown.[17−19] The PCET step in such light-triggered reactions provides almost a barrier-less access to desired products via either sequential or concerted ET−PT steps.[18,19] However, current examples usually utilize a long-lived triplet state which could force the PCET steps to compete with plethora of excited-state deactivation[18] and diffusion-limited loss pathways. Recently, Meyer and Papanikolas reported concerted ET−PT process through an intramolecular charge-transfer (CT) excitation of a hydrogen-bonded paranitrophenyl-phenol:*tert*-butylamine pair.[20] Elaborating on this idea, we propose that carrying out photoinduced PCET via singlet CT states under isolation would lead to successful implementation of novel photocatalytic schemes. According to our paradigm, photo-excited singlet states will provide the desired quantum and energy efficiency, while the confined environment will ensure kinetic stabilization of intermediates for subsequent diffusion-limited steps.

The reactive confinement of active sites in enzymes has been synthetically mimicked by water-soluble supramolecular host structures.[21−24] Molecular cages based on metal−organic frameworks[25−28] provide predefined chemical environment in solution for carrying out selective chemistry with desired efficiencies. Fujita et al. have previously reported a cationic octahedral Pd_6L_4 cage with N-donor ligands and open tetrahedral faces.[29] The group has demonstrated successful implementation of many organic transformations inside the cage with enhanced product selectivity, in addition to trapping unusual intermediates on the reaction pathway.[30] One of the unique features of this Pd_6L_4 cage is the propensity to generate host−guest CT states due to the presence of electron-deficient triazine walls.[31,32] The optical signatures of such host−guest CT states have often been used as evidence for incarceration of guest molecules.[33] Here we use the Pd-nanocage to actively host the anion radical state via the CT excitation and temporally couple a water-mediated PT step from an incarcerated guest molecule as depicted in Figure 1.

Our choice of guest molecules for carrying out the above conceptualized bidirectional PCET was inspired by the redox-active amino acid tyrosine in PSII. A phenol appendage to an electron-rich diphenylamine would ensure a photoreactive

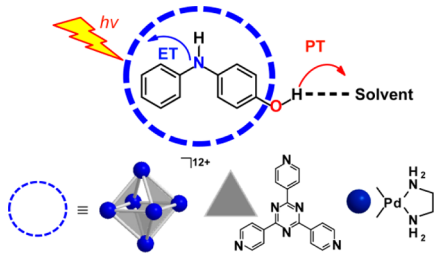

Figure 1. (top) Conceptual representation of photoinduced bidirectional PCET process inside a nanocage. (bottom) Chemical formula of the octahedral Pd_6L_4 nanocage; where L = 2,4,6-tri(4-pyridinyl)-1,3,5-triazine forms the tetrahedral faces, and ethylenediamine holds the Pd^{2+} ion.

Received: September 22, 2014
Published: October 21, 2014

dx.doi.org/10.1021/ja509761a | *J. Am. Chem. Soc.* 2014, 136, 15909−15912

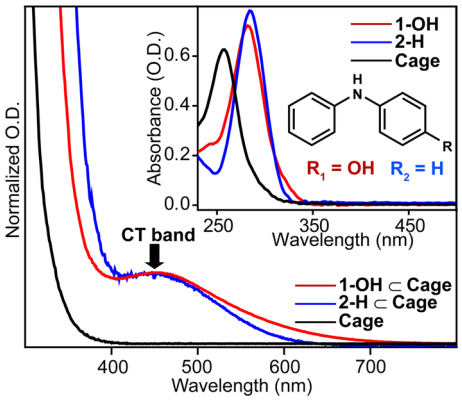

Figure 2. Solution spectra of **1-OH ⊂ cage** (red) and **2-H ⊂ cage** (blue) compared with absorption spectrum of empty Pd-cage in black. (Inset) Absorption spectra of free **1-OH** (red) and **2-H** (blue) along with the free cage (black) spectra.

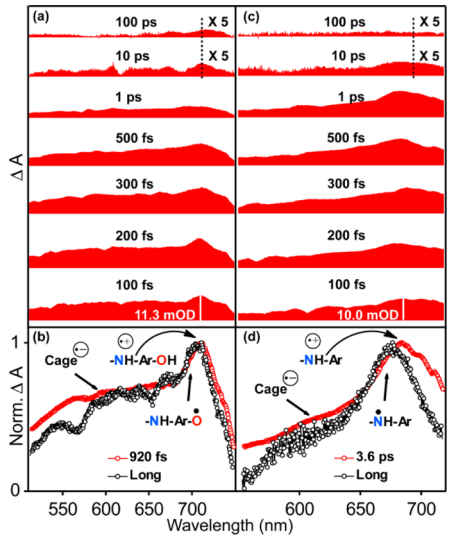

Figure 3. Time evoluton of the excited-state signal in the visible wavelengths and its corresponding SVD component spectra; (a,b) for **1-OH ⊂ cage**, (c,d) for **2-H ⊂ cage**. The traces at 10 and 100 ps were scaled 5 times for clarity.

molecule with an ionizable −OH group. Previous work showed successful incarceration of such amines in Pd_6L_4-type cages led to a broad absorption band in the visible region possibly associated with a CT transition.[34,35] We incarcerated 4-hydroxy-diphenylamine (**1-OH**) and diphenylamine (**2-H**) in order to test our hypothesis of the temporal coupling of the CT step with the PT reaction. Using broadband femtosecond transient absorption spectroscopy, we observed a ∼890 fs time scale for a solvent-coupled PT step in **1-OH** after photo-excitation at the host−guest CT band. The resulting solvent exposed phenoxyl radical is kinetically stabilized inside the cage and lives for >10 ns making it a potent intermediate for subsequent diffusion-limited reactions.

The Pd_6L_4 cage was synthesized using the synthetic route first reported by Fujita et al. (see Supporting Information).[29] Optimized incarceration of **1-OH** and **2-H** was carried out with a slightly modified procedure (Figures S1−S5) to ensure reproducibility. NMR quantification showed that ∼3 molecules of **1-OH** were inserted inside the cage similar to previously reported incarceration.[35] Steady state absorption spectra of free **1-OH** and **2-H** are shown in Figure 2 (inset) denotes the amine centric transition at ∼280 nm. Upon incarceration, new absorption bands corresponding to host-guest CT complex is observed which is centered at ∼460 nm. The absorption spectrum for the CT band in **1-OH ⊂ cage** extends until 720 nm, while for **2-H ⊂ cage** it decays off by 625 nm. These bands could not be reproduced by varying concentration of free amines in solution indicating specificity of the CT band for the host−guest complex. From NMR quantification of incarceration, we estimate a modest molar extinction coefficient of ∼1000 M^{-1} cm^{-1} for the CT band in **1-OH ⊂ cage**.

In order to show the CT character of the excited state and track its reactivity, we carried out femtosecond transient absorption spectroscopy with 490 nm excitation to selectively pump the optical CT band. Absorption transients were recorded at different pump−probe delays in the visible using a probe window ranging from 500 to 750 nm with an IRF of ∼100 fs. Figure 3a shows the evolution of the broad excited state absorption feature for **1-OH ⊂ cage** in water. The asymmetric ESA profile hinted at presence of at least two distinct species with one absorbing strongly at 710 nm. Pulse radiolysis study on free diphenylamine (DPA) has shown that the DPA radical cation absorbs at 700 nm, which closely resembles the observed 100 fs transient of incarcerated hydroxy-DPA.[36,37] However, the feature in between 450 and 600 nm appears broader than the previous report of the DPA radical cation spectrum. We assign the broad peak at ∼600 nm to the Pd_6L_4 cage localized anion radical which was first reported by Fujita et al. using steady illumination at low temperature.[38] The immediate appearance of both the hydroxy-DPA radical cation and the cage anion confirms our assignment of the optical CT state.

The spectral evolution of radical species in **1-OH ⊂ cage** shows rapid population decay within the first 10 ps evident from the remarkable intensity decay eventually leading to a new state which does not decay within the experimental time scale of 2 ns. To enumerate the spectra and lifetimes of the states, we carried out an SVD analysis to generate decay associated spectra from a sequential target model. Figure 3b shows the normalized component spectra with 920 fs and nondecaying lifetime, respectively. The short component spectrum resembles an additive spectrum of the **1-OH** localized radical cation and a cage localized anion radical feature. The nondecaying component is slightly narrow on the red edge but retains the overall shape of the 920 fs component. Although amplitude of the nondecaying component is almost ∼2% of the original radical cation spectrum, it could still be detected sensitively in our measurements (Figure S13). The small absorption signal of the nondecaying state can be explained by a loss in absorption cross-section upon formation of a neutral radical. Previous electrochemical measurements have shown ∼9−10 times decrease in the molar extinction coefficients of free DPA cation radical upon its conversion to neutral radical via deprotonation.[36] We independently confirmed the deprotonation step by carrying out nanosecond flash photolysis which generated photoproduct species at 10 ns having major absorption at ∼395 nm (Figure S12) and a weak broad feature between 550 and 700 nm, matching very well with other known phenoxyl radical species.[39] Additionally, kinetic fitting at 715 nm showed a minor (∼2%) decay component of ∼7.75 ps, which possibly indicates small heterogeneity in the deprotonation step (Figure S14 and Table ST1). Therefore, the major spectral evolution within the CT state indicates an ultrafast PT step to a proximal base, assigned to be an associated water molecule. Our assignment is supported by the crystal structure of the **1-OH ⊂**

dx.doi.org/10.1021/ja509761a | J. Am. Chem. Soc. 2014, 136, 15909−15912

$[Co_6L_4(SCN)_2]_m$ which shows protrusion of the −OH group toward the solvent.[35]

In order to address if deprotonation can only occur through solvent exposed −OH or also from the interior −NH functionality, we optically excited the CT state of **2-H ⊂ cage** in water. The ESA spectral evolution shown in Figure 3c is interpreted within the same framework as proposed above for the incarcerated **1-OH** molecule. The radical cation spectrum seen immediately after photo-excitation evolves to a nondecaying state although with a slower time scale. SVD analysis of the **2-H** incarcerated cage, presented in Figure 3d, shows the radical cation component with maxima at 690 nm and ∼10 nm blue-shifted neutral radical spectrum. The 3.6 ps lifetime of the radical cation implies almost 3−4 times slower deprotonation step, although kinetic fitting shows two time constants of ∼2.4 ps (major) and ∼15.5 ps (minor) respectively (Table ST3). We assign the minor component to a photochemically incompetent fraction that shows only CT recombination, time scale supported independently by measurements on tertiary amine guests (Figure S15 in SI). Thus, for **2-H ⊂ cage,** the PT rate slows down possibly due to the buried −NH moiety, although the access to proton accepting water molecule is not completely blocked. The PT time scales therefore are set up by the kinetic accessibility of the water molecule along with the corresponding pK_a of the ionizable group. The obvious distinction in temporal delay of the PT step in **1-OH** and **2-H** motivates us to interrogate the differences in solvation dynamics of the two host−guest systems and derive an understanding of the nature of the coupling.

We interrogated the solvation dynamics by optically triggering a large dipole moment change across the host−guest system through the CT state. Broadband femtosecond near-IR dynamics were recorded using a white light continuum probe ranging from 850 to 1300 nm to capture the radical-cage coupled CT state (Figure S7). The dipolar CT state is delocalized over the entire supramolecular system and thereby triggers the inertial water rearrangement around the host−guest complex. For the **1-OH ⊂ cage** we observe a measurable blue shift of ∼280 cm^{-1} of the ESA band (Figure S9) within 500 fs implying partial solvation, before the loss of ESA signal due to the PT step. However, continuous solvation until 1 ps for **2-H ⊂ cage** without an evident PT implies possibly larger rearrangement of solvent shell is required for the PT step. The lifetime components obtained after an SVD analysis (Figure 4a inset) showed ∼670 cm^{-1} spectral blue-shift upon deprotonation of **1-OH**. This shift in ESA feature can be explained by stabilization of the deprotonated state via electronic conjugation and solvation. The smaller shift of ∼510 cm^{-1} (Figure 4b inset) seen in the case of **2-H ⊂ cage** is possibly due to the buried −NH group. Therefore, the guest sensitive CT ESA feature can act as a probe to track chemical events inside the Pd_6L_4-nanocage.

To establish unequivocal validity of the PCET process, isotope dependence of the PT step was experimentally measured. Figure 4a,b shows the ESA decay kinetics at 715 nm which represents the decay of the radical cation population for both **1-OH ⊂ cage** and **2-H ⊂ cage** in both H_2O and D_2O respectively. The major amplitude in the **1-OH ⊂ cage** decay dynamics is attributed to a ∼890 fs component in H_2O while ∼1.17 ps time constant in D_2O (Figure 4a). The kinetic isotope effect (KIE) of 1.32 confirms the PT step after CT excitation. The minor component of ∼7.75 ps in H_2O slows down to ∼15.8 ps in D_2O indicating a large KIE value of ∼2.05, which possibly implies increased proton donor−acceptor distances.[5] Upon comparison with **2-H ⊂ cage** which revealed a KIE value of 1.72 (shown in Figure 4b) due to buried

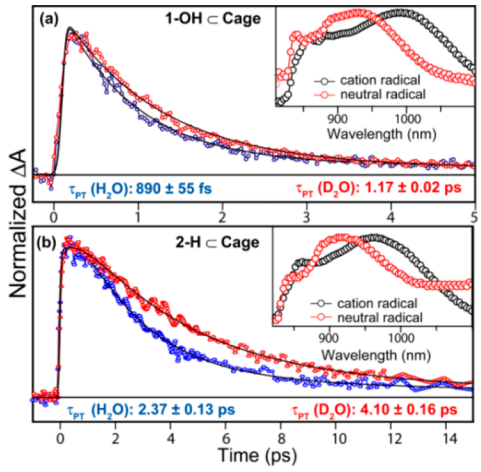

Figure 4. Decay kinetics at 715 nm for the radical cation feature in (a) **1-OH ⊂ cage** and (b) **2-H ⊂ cage**, respectively, in D_2O (red circles) and H_2O (blue circles). (Insets) Spectral decomposition of NIR femtosecond transients representing the protonated and deprotonated CT state in (a) **1-OH ⊂ cage** and (b) **2-H ⊂ cage**.

N−H deprotonation, we assign the minor component in **1-OH ⊂ cage** to a proton removal from the N−H site. In order to rule out any ambiguity in our interpretation of the PT step from experimental KIE values,[40] we carried out isotope exchange measurements on *N*-methyldiphenylamine (**3-NMe**) incarcerated cage which does not have any ionizable proton. The KIE of ∼1.09 (Figures S10 and S11) indicates the validity of our PT assignment. Our results thus indicate two plausible PT channels for **1-OH** and one PT step for **2-H** in cage.

In Figure 5, we summarize the first demonstration of an ultrafast light-induced PCET reaction inside a nanocage using a chemical scheme. The ground state of the incarcerated **1-OH** shows a direct interaction with the water molecule. Triggering a large dipole moment change via host−guest CT excitation reorients the solvent water to achieve an optimized reactive geometry. This dynamic reorientation initiates the proton movement toward the water molecule and thereby producing a neutral phenoxyl radical which lives longer than 10 ns. Although majority of the PCET process occurs through the phenol end, a minor tautomer does contribute to the excited-state heterogeneity leading to much slower N−H deprotonation with a large KIE. The support for this pathway emerges from the similarity in KIE values observed for N−H deprotonation in **2-H ⊂ cage**, although a much slower PT time scale in **1-OH** may indicate altered solvation structure or dynamics. To our knowledge the time scale of the entire bidirectional PCET step for **1-OH ⊂ cage** is the fastest measured coupled electron−proton event and is only 4 times slower than the photo-EPT reported by Meyer and Papanikolas.[20] The yield of the reaction is dictated by the CT recombination rates which are typically ∼5−20 ps for aprotic tertiary amine guests much slower than the PT pathway. The separation of time scales guarantees almost >80% quantum yield for the PCET product, reminiscent of photosynthetic control of Y_z radical formation. Our results should motivate new experimental and computational efforts to unravel the precise nature of the solvent coordinate and host coupling to the PCET process.

In conclusion, we show that photochemical reactions can be driven within nanoscopic molecular cages using host−guest CT excitation. We provide the first proof-of-concept result by demonstrating the fastest bidirectional photoinduced PCET

dx.doi.org/10.1021/ja509761a | J. Am. Chem. Soc. 2014, 136, 15909−15912

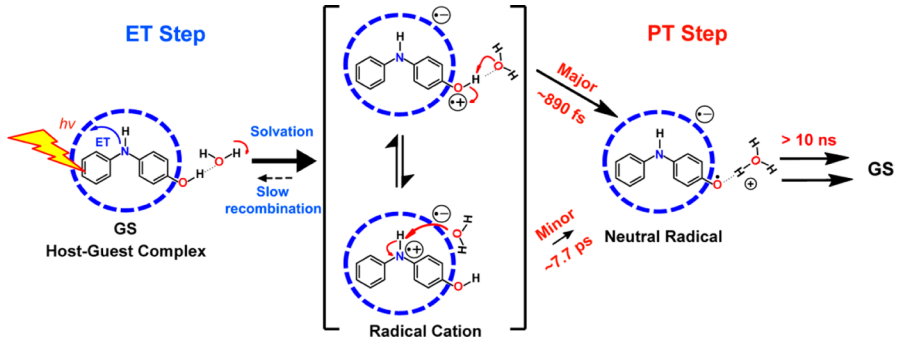

Figure 5. Scheme for photoinduced PCET inside a Pd_6L_4 nanocage driven by optical excitation of host–guest CT state.

reaction known for a sequential process. Using time-resolved pump–probe spectroscopy we provide direct evidence for the protonated radical cation, neutral radical, and the cage anion species as the reaction proceeds on the singlet excited surface. The long lifetime of the photoproduced neutral phenoxyl radical should help initiate redox chemistry in the diffusion-controlled time scales. The presented paradigm for triggering redox reactions can be generalized by choosing complementary host–guest pairs in order to generate an optical CT band. We envision that tuning the host–guest electronics will lead to larger optical cross-section of the CT band and thereby could eliminate the need for external photosensitizers in photocatalysis.

■ ASSOCIATED CONTENT

Supporting Information

Details of synthesis and additional time-resolved data. This material is available free of charge via the Internet at http://pubs.acs.org.

■ AUTHOR INFORMATION

Corresponding Author

dasgupta@tifr.res.in

Notes

The authors declare no competing financial interest.

■ ACKNOWLEDGMENTS

Authors thank Mr. Palas Roy and Ms. K. Vijaya Lakshmi (TIFR) for discussions; and Dr. Rajib Ghosh and Dr. Dipak Palit (BARC, Trombay) for flash photolysis measurements. National NMR facility at TIFR is acknowledged. J.D. thanks Department of Atomic Energy, India for monetary support.

■ REFERENCES

(1) Cukier, R. I.; Nocera, D. G. *Annu. Rev. Phys. Chem.* **1998**, *49*, 337–369.
(2) Mayer, J. M. *Annu. Rev. Phys. Chem.* **2004**, *55*, 363–390.
(3) Bonin, J.; Costentin, C.; Robert, M.; Savéant, J.-M.; Tard, C. *Acc. Chem. Res.* **2011**, *45*, 372–381.
(4) Weinberg, D. R.; Gagliardi, C. J.; Hull, J. F.; Murphy, C. F.; Kent, C. A.; Westlake, B. C.; Paul, A.; Ess, D. H.; McCafferty, D. G.; Meyer, T. J. *Chem. Rev.* **2012**, *112*, 4016–4093.
(5) Hammes-Schiffer, S.; Stuchebrukhov, A. A. *Chem. Rev.* **2010**, *110*, 6939–6960.
(6) Dasgupta, J.; van Willigen, R. T.; Dismukes, G. C. *Phys. Chem. Chem. Phys.* **2004**, *6*, 4793–4802.
(7) Mukhopadhyay, S.; Mandal, S. K.; Bhaduri, S.; Armstrong, W. H. *Chem. Rev.* **2004**, *104*, 3981–4026.
(8) McEvoy, J. P.; Brudvig, G. W. *Chem. Rev.* **2006**, *106*, 4455–4483.
(9) Meyer, T. J.; Huynh, M. H. V.; Thorp, H. H. *Angew. Chem., Int. Ed.* **2007**, *46*, 5284–5304.
(10) Chang, C. J.; Loh, Z.-H.; Shi, C.; Anson, F. C.; Nocera, D. G. *J. Am. Chem. Soc.* **2004**, *126*, 10013–10020.
(11) Sjödin, M.; Styring, S.; Wolpher, H.; Xu, Y.; Sun, L.; Hammarström, L. *J. Am. Chem. Soc.* **2005**, *127*, 3855–3863.
(12) Moore, G. F.; et al. *J. Am. Chem. Soc.* **2008**, *130*, 10466–10467.
(13) Warren, J. J.; Mayer, J. M. *J. Am. Chem. Soc.* **2011**, *133*, 8544–8551.
(14) Swierk, J. R.; Mallouk, T. E. *Chem. Soc. Rev.* **2013**, *42*, 2357–2387.
(15) Zhang, M. T.; Irebo, T.; Johansson, O.; Hammarstrom, L. *J. Am. Chem. Soc.* **2011**, *133*, 13224–13227.
(16) Megiatto, J. D., Jr.; et al. *Nat. Chem.* **2014**, *6*, 423–428.
(17) Concepcion, J. J.; et al. *J. Am. Chem. Soc.* **2007**, *129*, 6968–6969.
(18) Wenger, O. S. *Acc. Chem. Res.* **2013**, *46*, 1517–1526.
(19) Eisenhart, T. T.; Dempsey, J. L. *J. Am. Chem. Soc.* **2014**, *136*, 12221–12224.
(20) Westlake, B. C.; et al. *Proc. Natl. Acad. Sci. U.S.A.* **2011**, *108*, 8554–8558.
(21) Iwasawa, T.; Mann, E.; Rebek, J. *J. Am. Chem. Soc.* **2006**, *128*, 9308–9309.
(22) Yoshizawa, M.; Klosterman, J. K.; Fujita, M. *Angew. Chem., Int. Ed.* **2009**, *48*, 3418–3438.
(23) Smulders, M. M. J.; Nitschke, J. R. *Chem. Sci.* **2012**, *3*, 785–788.
(24) Hart-Cooper, W. M.; Clary, K. N.; Toste, F. D.; Bergman, R. G.; Raymond, K. N. *J. Am. Chem. Soc.* **2012**, *134*, 17873–17876.
(25) Chakrabarty, R.; Mukherjee, P. S.; Stang, P. J. *Chem. Rev.* **2011**, *111*, 6810–6918.
(26) Leininger, S.; Olenyuk, B.; Stang, P. J. *Chem. Rev.* **2000**, *100*, 853–907.
(27) Seidel, S. R.; Stang, P. J. *Acc. Chem. Res.* **2002**, *35*, 972–983.
(28) Stang, P. J.; Olenyuk, B. *Acc. Chem. Res.* **1997**, *30*, 502–518.
(29) Fujita, M.; Oguro, D.; Miyazawa, M.; Oka, H.; Yamaguchi, K.; Ogura, K. *Nature* **1995**, *378*, 469–471.
(30) Inokuma, Y.; Kawano, M.; Fujita, M. *Nat. Chem.* **2011**, *3*, 349–358.
(31) Furutani, Y.; Kandori, H.; Kawano, M.; Nakabayashi, K.; Yoshizawa, M.; Fujita, M. *J. Am. Chem. Soc.* **2009**, *131*, 4764–4768.
(32) Han, L.; Qin, L.; Xu, L.-P.; Zhao, W.-N. *Inorg. Chem.* **2013**, *52*, 1667–1669.
(33) Bruns, C. J.; Fujita, D.; Hoshino, M.; Sato, S.; Stoddart, J. F.; Fujita, M. *J. Am. Chem. Soc.* **2014**, *136*, 12027–12034.
(34) Inokuma, Y.; Arai, T.; Fujita, M. *Nat. Chem.* **2010**, *2*, 780–783.
(35) Inokuma, Y.; Kojima, N.; Arai, T.; Fujita, M. *J. Am. Chem. Soc.* **2011**, *133*, 19691–19693.
(36) Schmidt, K. H.; Bromberg, A.; Meisel, D. *J. Phys. Chem.* **1985**, *89*, 4352–4357.
(37) Maroz, A.; Hermann, R.; Naumov, S.; Brede, O. *J. Phys. Chem. A* **2005**, *109*, 4690–4696.
(38) Yoshizawa, M.; Miyagi, S.; Kawano, M.; Ishiguro, K.; Fujita, M. *J. Am. Chem. Soc.* **2004**, *126*, 9172–9173.
(39) Chang, C. J.; Chang, M. C. Y.; Damrauer, N. H.; Nocera, D. G. *Biochim. Biophys. Acta, Bioenerg.* **2004**, *1655*, 13–28.
(40) Kuss-Petermann, M.; Wenger, O. S. *J. Phys. Chem. Lett.* **2013**, *4*, 2535–2539.